

Investigating Supergiant Fast X-ray Transients with LOFT

P. Romano*, E. Bozzo[†], P. Esposito**, C. Ferrigno[†] and V. Mangano*

*INAF - IASF Palermo, Via U. La Malfa 153, I-90146 Palermo, Italy

[†]ISDC, University of Geneva, Chemin d'Écogia 16, 1290 Versoix, Switzerland

**INAF - IASF Milano, Via E. Bassini 15, I-20133 Milano, Italy

Abstract. Supergiant Fast X-ray Transients (SFXT) are a class of High-Mass X-ray Binaries whose optical counterparts are O or B supergiant stars, and whose X-ray outbursts are about 4 orders of magnitude brighter than the quiescent state. LOFT, the Large Observatory For X-ray Timing, with its coded mask Wide Field Monitor (WFM) and its 10 m² class collimated X-ray Large Area Detector (LAD), will be able to dramatically deepen the knowledge of this class of sources. It will provide simultaneous high S/N broad-band and time-resolved spectroscopy in several intensity states, and long term monitoring that will yield new determinations of orbital periods, as well as spin periods. We show the results of an extensive set of simulations performed using previous observational results on these sources obtained with *Swift* and *XMM-Newton*. The WFM will detect all SFXT flares within its field of view down to a 15–20 mCrab in 5 ks. Our simulations describe the outbursts at several intensities ($F_{(2-10\text{keV})} = 5.9 \times 10^{-9}$ to 5.5×10^{-10} erg cm⁻² s⁻¹), the intermediate and most common state (10^{-11} erg cm⁻² s⁻¹), and the low state (1.2×10^{-12} to 5×10^{-13} erg cm⁻² s⁻¹). We also considered large variations of N_{H} and the presence of emission lines, as observed by *Swift* and *XMM-Newton*.

Keywords: Missions – X-rays: binaries – X-rays: individual: IGR J16479–4514

PACS: 95.55.Ka – 97.80.Jp – 98.70.Qy

PERSPECTIVES FOR SUPERGIANT FAST X-RAY TRANSIENTS

Supergiant fast X-ray transients (SFXTs) are High-Mass X-ray Binaries (HMXB) transients that show flares peaking at 10^{36} – 10^{37} erg s⁻¹ (2–10 keV observed flux of 10^{-9} erg cm⁻² s⁻¹) lasting a few hours. Their X-ray spectra during a flare are similar to those of accreting neutron stars, and can be described as a flat power-law below ~ 10 keV sometimes displaying a cutoff at 15–30 keV. Their large X-ray dynamic range (3–5 orders of magnitude) and their association with OB supergiant companions make them a peculiar class of HMXBs that now include about 10 SFXTs and 10 candidates (showing the same X-ray properties but still lacking an optical spectroscopic classification).

LOFT, the Large Observatory For X-ray Timing [1], is a newly proposed space mission selected by ESA in February 2011 as one of the four M3 mission candidates that will compete for a launch opportunity at the start of the 2020s. The LOFT Large Area Detector [LAD, 2] has an effective area a factor of ~ 20 larger than RXTE/PCA (the largest area X-ray instrument ever flown) and much improved energy resolution (better than 260 eV). It is specifically designed to exploit the diagnostics of very rapid X-ray flux and spectral variability that directly probe the motion of matter down to distances very close to black holes and neutron stars. The LOFT Wide Field Monitor [WFM, 3]

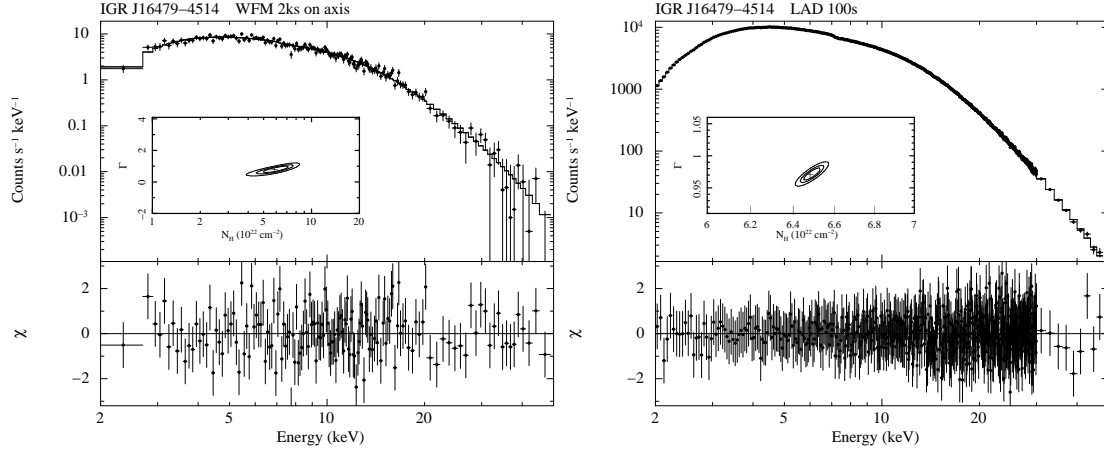


FIGURE 1. Simulated LOFT spectra of IGR J16479–4514 with an absorbed power-law model with a cut-off [5, $N_{\text{H}} = 6.5 \times 10^{22} \text{ cm}^{-2}$, $\Gamma = 0.98$, $E_{\text{c}} = 13.5 \text{ keV}$, $F_{(2-10\text{keV})} = 5.9 \times 10^{-9} \text{ erg cm}^{-2} \text{ s}^{-1}$]. *Left panel:* WFM spectrum (2 ks). *Right panel:* LAD spectrum (100 s).

will discover and localise X-ray transients and impulsive events and monitor spectral state changes with unprecedented sensitivity, providing interesting targets for LAD’s pointed observations. Through the LOFT Burst Alert System (LBAS), the position and occurrence time of bright and impulsive events discovered by the WFM will be transmitted on the ground within about 30 s from detection.

The LOFT contribution to the SFXT investigation will include unprecedented simultaneous high S/N broad-band and time-resolved spectroscopy in several intensity states. Starting point for our simulations were *Swift* broad-band observations and detailed *XMM-Newton* observations that describe the outburst state at several intensities ($F_{(2-10\text{keV})} = 5.9 \times 10^{-9}$ to $5.5 \times 10^{-10} \text{ erg cm}^{-2} \text{ s}^{-1}$), the intermediate (and most common, $F_{(2-10\text{keV})} = 10^{-11} \text{ erg cm}^{-2} \text{ s}^{-1}$) state, and low state ($F_{(2-10\text{keV})} = 1.2 \times 10^{-12}$ to $5 \times 10^{-13} \text{ erg cm}^{-2} \text{ s}^{-1}$). In our simulations we also considered large variations of N_{H} and the presence of emission lines, also as observed by *Swift* and *XMM-Newton*. For the WFM we used ‘on axis’ ARF, RMF and the background model of Gruber et al. [4], for the 1.5D camera. For the LAD we used the ‘requirements’ (v4) ARF, RMF, and background¹.

SFXTs with the WFM

The sensitive, long term monitoring with the WFM will yield new determinations of the SFXT orbital period P_{orb} . Our simulations show that the WFM will also be able to detect all SFXT short flares within its field of view (FOV) down to a 15–20 mCrab in 5 ks. The calculation of the percentage of SFXT outbursts/flares observed instantaneously in the WFM FOV is under investigation.

¹ User guides at: <http://www.isdc.unige.ch/loft/>, under Responses.

The WFM is ideal to catch bright outbursts that reach $6 \times 10^{-9} \text{ erg cm}^{-2} \text{ s}^{-1}$: we obtain $\Delta N_{\text{H}}/N_{\text{H}}$ and $\Delta \Gamma/\Gamma$ within $\sim 30\%$ in 1 ks, within $\sim 20\%$ in 2 ks (such intense fluxes are maintained for a few ks only, so there is no point in investigating longer integrations). For intermediate flares ($F_{(2-10\text{keV})} = 10^{-9} \text{ erg cm}^{-2} \text{ s}^{-1}$) we obtain $\Delta N_{\text{H}}/N_{\text{H}}$ and $\Delta \Gamma/\Gamma \gtrsim 50\%$ in 5 ks, while flares with fluxes lower than $F_{(2-10\text{keV})} = 10^{-9} \text{ erg cm}^{-2} \text{ s}^{-1}$ might require longer exposure times to have sufficiently detailed measurements of the source spectral parameters. Furthermore, we need $N_{\text{H}} \gtrsim 5 \times 10^{22} \text{ cm}^{-2}$ to constrain it adequately, given the 2 keV threshold with exposure times as low as 2–5 ks. In Fig. 1 (left), we show a 2 ks simulated WFM spectrum of the SFXT IGR J16479–4514 as observed by *Swift* [5], an absorbed power-law model with a cut-off ($N_{\text{H}} = 6.5 \times 10^{22} \text{ cm}^{-2}$, $\Gamma = 0.98$, $E_{\text{c}} = 13.5 \text{ keV}$, $F_{(2-10\text{keV})} = 5.9 \times 10^{-9} \text{ erg cm}^{-2} \text{ s}^{-1}$).

SFXTs with the LAD

The LAD is best suited for pointed observations and re-pointing to lower fluxes, and line spectroscopy. One may be lucky to catch bright outbursts ($F_{(2-10\text{keV})} = 6 \times 10^{-9} \text{ erg cm}^{-2} \text{ s}^{-1}$) which will yield excellent time-resolved spectroscopy (down to 1 s) with $\Delta N_{\text{H}}/N_{\text{H}}$ and $\Delta \Gamma/\Gamma$ within $\sim 1\%$ in 200 s. In Fig. 1 (right), we show a 100 s LAD simulated spectrum of IGR J16479–4514. Intermediate flares will yield $\Delta N_{\text{H}}/N_{\text{H}}$ and $\Delta \Gamma/\Gamma$ within $\sim 5\%$ in 1 ks for low N_{H} ($F_{(2-10\text{keV})} \sim 9 \times 10^{-10} \text{ erg cm}^{-2} \text{ s}^{-1}$), $\Delta N_{\text{H}}/N_{\text{H}}$ and $\Delta \Gamma/\Gamma$ within $\sim 5\%$ in 1 ks ($F_{(2-10\text{keV})} = 5 \times 10^{-10} \text{ erg cm}^{-2} \text{ s}^{-1}$). Far more likely will be the case of the intermediate state [6] characterized by fluxes of $F_{(2-10\text{keV})} = 10^{-11} \text{ erg cm}^{-2} \text{ s}^{-1}$. Emission lines can be recovered quite nicely, as shown in Fig. 2 by the 1 ks simulated spectrum of IGR J16479–4514 in quiescence [7, note that the exposure time of the *XMM-Newton* data where the iron line was found was of 28 ks]. Low intensity states down to $F_{(2-10\text{keV})} = 1.2 \times 10^{-12} \text{ erg cm}^{-2} \text{ s}^{-1}$ can be studied in 10 ks.

Pulsed Fractions

Several SFXTs are X-ray pulsars (with $P_{\text{spin}} \sim 4\text{--}2000 \text{ s}$) so it is paramount to determine if all of them are indeed pulsating sources and to what limit we can determine P_{spin} for the whole sample. In conjunction with the WFM monitoring, this should in turn allow us to address the issue of why SFXTs differ from ordinary HMXBs with the same P_{orb} and P_{spin} . In particular, we investigated whether we can measure pulsations during the bright outbursts with the WFM, and the required length of the pointed LAD observations to accurately measure a P_{spin} . We assumed a sinusoidal pulse profile and Fourier transform searches with $2^{23}\text{--}2^{24}$ sampled frequencies. From known discrete Fourier transform properties, the relationship between the pulsed fraction PF of the smallest detectable signal and the number of counts is given by $\text{PF} \propto (N_{\text{ph}})^{-1/2}$. Based on our spectral simulations, we expect to be able to detect signals with pulsed fraction as

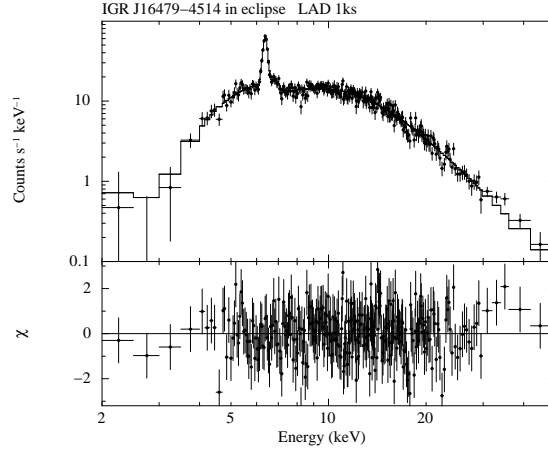


FIGURE 2. LAD simulated spectrum (1 ks) of IGR J16479–4514 during eclipse [7, $N_{\text{H}} = 35.2 \times 10^{22} \text{ cm}^{-2}$, $\Gamma = 0.98$, $\text{Norm}(K_{\alpha}) = 4.6 \times 10^{-5} \text{ ph cm}^{-2} \text{ s}^{-1}$, $F_{(2-10\text{keV})} = 10^{-11} \text{ erg cm}^{-2} \text{ s}^{-1}$].

TABLE 1. Pulsed fractions as a function of flux.

	$F_{(2-10\text{keV})} \text{ (erg cm}^{-2} \text{ s}^{-1})$	%
WFM (5ks)	6×10^{-9}	2.4 (5σ)
	6×10^{-10}	66 (5σ), 56 (3σ)
LAD	6×10^{-9}	0.08 (5 ks, 5σ)
	6×10^{-10}	0.3 (5 ks, 5σ)
	1×10^{-12}	53.4 (10 ks, 3σ)

low as those reported in Table 1. Note that red noise, not accounted for in our simulations yet, might lower the sensitivity toward the longer periods.

ACKNOWLEDGMENTS

We acknowledge financial contribution from the contract ASI-INAF I/004/11/0.

REFERENCES

1. M. Feroci, L. Stella, M. X. van der Klis, et al. *Experimental Astronomy* p. 100 (2011), 1107.0436.
2. S. Zane, D. Walton, T. X. Kennedy, et al. *ArXiv e-prints* (2012), 1209.1498.
3. S. Brandt, M. Hernanz, L. X. Alvarez, et al. *ArXiv e-prints* (2012), 1209.1499.
4. D. E. Gruber, J. L. Matteson, L. E. Peterson, and G. V. Jung, *ApJ* **520**, 124–129 (1999), arXiv: astro-ph/9903492.
5. P. Romano, L. Sidoli, V. Mangano, S. Vercellone, J. A. Kennea, G. Cusumano, H. A. Krimm, D. N. Burrows, and N. Gehrels, *ApJL* **680**, L137–L140 (2008), arXiv:0805.2089.
6. P. Romano, V. La Parola, S. Vercellone, G. Cusumano, L. Sidoli, H. A. Krimm, C. Pagani, P. Esposito, E. A. Hoversten, J. A. Kennea, K. L. Page, D. N. Burrows, and N. Gehrels, *MNRAS* **410**, 1825–1836 (2011), 1009.1146.
7. E. Bozzo, L. Stella, G. Israel, M. Falanga, and S. Campana, *MNRAS* **391**, L108–L112 (2008), 0809.3642.